01 Jul 2019

Multicenter Distorted-Wave Approach for Electron-Impact Ionization of Molecules

Esam Ali

Don H. Madison
Missouri University of Science and Technology, madison@mst.edu

Multicenter distorted-wave approach for electron-impact ionization of molecules

Esam Ali and Don Madison
Department of Physics, Missouri University of Science and Technology, Rolla, Missouri 65409, USA

(Received 8 February 2019; revised manuscript received 7 April 2019; published 31 July 2019)

We have previously used the molecular three-body distorted-wave model to examine electron-impact single ionization of molecules. One of the possible weaknesses of this approach lies in the fact that the continuum electron wave functions do not depend on the orientation of the molecule. Here we introduce a model called the multicenter molecular three-body distorted-wave (MCM3DW) approach, for which the continuum electron wave functions depend on the orientation of the molecule at the time of ionization. The MCM3DW results are compared with experimental data taken from work by Dorn and colleagues [Ren *et al.*, Phys. Rev. A **91**, 032707 (2015); **93**, 062704 (2016); **95**, 022701 (2017); Phys. Rev. Lett. **109**, 123202 (2012); Gong *et al.*, Phys. Rev. A **98**, 042710 (2018)] in which they measured triple differential cross sections for single ionization of molecular hydrogen while simultaneously determining the orientation of the H_2^+ ion at the time of ionization. Comparisons are also made with previous theoretical calculations. It is found that orientation effects are important for low incident energy electrons. Very nice agreement with experiment and the time-dependent close coupling results is found for an incident electron energy of 26 eV. Orientation effects become relatively unimportant by the time the incident electron energy is 54 eV.

DOI: 10.1103/PhysRevA.100.012712

I. INTRODUCTION

One of the most fundamental unresolved problems in physics is the few-body problem and the simplest few-body problem is the three-body problem. Since there is no known analytic solution of the Schrödinger equation for three particles, numerical approximations have to be made whose validity can only be tested by comparing with experimental data. One of the best testing grounds for theoretical approximations is single ionization of targets by charged particle impact. The most sensitive test of theory is obtained by comparing with the most detailed experimental data. For charged particle single ionization of targets, the most detailed experiments determine the energy and angular location of all three final-state particles and the measured cross sections are normally called either the fully differential cross sections or more commonly the triply differential cross sections (TDCS) in spite of the fact that the cross sections are actually fivefold differential.

For electron-impact ionization of atoms, three different close coupling approximations have been developed which yield excellent agreement with experimental data for ionization of atomic hydrogen and helium—the convergent close coupling (CCC) developed by Bray and Stelbovics [1], the time-dependent close coupling approximation (TDCC) developed by Colgan and Pindzola [2], and the exterior complex scaling (ECS) developed by Rescigno *et al.* [3]. For larger atoms, it has recently been shown that the *R*-matrix method with pseudostates developed by Zatsarinny and Bartschat yields good agreement with experiment for ionization of neon [4] and argon [5].

Theoretical progress in treating ionization of molecules has been much slower due to the additional complexity of multicenter nuclei. The CCC approach [6], the *R* matrix with pseudostates (RMPS) approach [7], and the TDCC approach [8] have been applied to the calculation of total cross sections for electron-impact ionization of H_2, and all three methods yielded excellent agreement with experiment. The TDCC approach has also been adapted to treat the TDCS for ionization of H_2 [9,10], but to date no close coupling method has been developed for larger molecules. The most versatile theoretical approach for treating more complex targets is the distorted-wave Born approximation (DWBA) method. We introduced the three-body distorted-wave (3DW) method for electron-impact ionization of atoms. This approach is a standard DWBA with the addition of including the postcollision interaction (PCI) exactly to all orders of perturbation theory. Normally one would expect that a DWBA approach would be appropriate for higher energies but not low energies. However, it was recently shown that including PCI exactly yielded very good agreement with experiment (as good as the *R* matrix with pseudostates) for low-energy ionization of neon [4]. However, the agreement was not as good for ionization of argon [5].

For the case of molecules, we have developed the molecular three-body distorted-wave (M3DW) approximation [11] and we have used this method to investigate ionization of several different targets. This method is fully numerical which means that a numerical six-dimensional (6D) integral must be performed to calculate the TDCS for a single orientation of the molecule. The fact that we need to do a full 6D integral stems from the fact that we include PCI exactly. Not doing so reduces the integral to a two-dimensional (2D) integral and orders of magnitude less computer time! Since most of the experimental measurements do not determine the orientation of the molecule at the time of ionization, an average over all orientations needs to be performed. When we first started this work, we did not have the computational resources to be able to perform a proper average so we introduced the orientation averaged molecular orbital (OAMO) approximation [12–15].

This approximation yielded qualitative agreement with experiment in some cases but, unfortunately, overall was not a very good approximation. It seems to work better for the larger molecules but does not predict the detailed structure seen in the data. More recently, we have been able to perform calculations using the proper average over orientations and this approach yields much better agreement with experiment.

One of the potential shortcomings of the M3DW method lies in the fact that the distorted waves for the continuum electrons are calculated using a spherically symmetric distorting potential which means that the distorted waves do not depend on the orientation of the molecule which might potentially be important. Very recently, Gong *et al.* [16] introduced a multicenter three distorted-wave approach (MCTDW) for which the distorted waves depend on the orientation of the molecule. To solve the multicenter Schrödinger equation, the single-center expansion method [17–19] was used to expand the wave functions and potentials. This procedure results in a set of coupled differential equations and the off-diagonal terms were ignored which yields a set of decoupled partial-wave equations. They applied the method to electron-impact ionization of water and overall found somewhat better agreement with experiment than the M3DW [20]. One of the possible drawbacks of the MCTDW method is that the postcollision interaction (PCI) between the two outgoing electrons is approximated using the Ward-Macek [21] approximation while the M3DW contains PCI exactly to all orders of perturbation theory.

The purpose of this paper is to introduce an updated version of the M3DW for which the distorted waves depend on the orientation of the molecule—a multicenter M3DW (MCM3DW). Although it can be applied to molecules of any size, here we consider ionization of molecular hydrogen. The idea behind our approach is to form the distorted wave as a product of distorted waves for each atom in the molecule which depends on the exact location of the atom. The theory is described in Sec. II. In Sec. III, we compare the MCM3DW results with experimental measurements for ionization of H_2 for the case in which the orientation of the molecule at the time of ionization was determined [22]. This is a sevenfold differential cross section and should represent the most sensitive possible test for theory. The MCM3DW results are also compared with M3DW as well as TDCC theoretical results.

II. THEORY

A. M3DW

The multicenter approach proposed here is an extension of the M3DW model which is described more fully in Refs. [11–15] so only a brief outline of the theory will be presented. This is a fully quantum mechanical approach and the direct scattering T matrix $T_{\rm dir}$ is given by

$$T_{\rm dir}(\mathbf{R}) = \langle \chi_1^-(\mathbf{k}_1,\mathbf{r}_1)\chi_2^-(\mathbf{k}_2,\mathbf{r}_2)C_{12}(\mathbf{r}_{12})|V_i - U_i|\psi_{Dy}(\mathbf{r}_2,\mathbf{R})\chi_i^+(\mathbf{k}_i,\mathbf{r}_1)\rangle, \quad (1)$$

where $\chi_i^+(\mathbf{k}_i,\mathbf{r}_1)$ is the initial-state continuum distorted for the incoming electron with momentum $\mathbf{k}_i$ and the (+) indicates outgoing wave boundary conditions. The factors $\chi_1^-(\mathbf{k}_1,\mathbf{r}_1)$ and $\chi_2^-(\mathbf{k}_2,\mathbf{r}_2)$ are the scattered and ejected electron distorted waves with momentum $\mathbf{k}_1$ and $\mathbf{k}_2$ satisfying incoming wave boundary conditions, the factor $C_{12}(\mathbf{r}_{12})$ is the final-state Coulomb interaction between the two outgoing electrons—normally called the postcollision interaction (PCI), and $\psi_{Dy}(\mathbf{r}_2,\mathbf{R})$ is the initial-state Dyson molecular wave function which depends on the orientation of the molecule $\mathbf{R}$. Al-Hagan *et al.* [23] showed that molecular cross sections for H_2 evolve into atomic cross sections for He as the internuclear separation goes to zero. The position vectors $(\mathbf{r}_1,\mathbf{r}_2)$ are the coordinates with respect to the center of mass (c.m.). Please note that we use the subscript 1 to designate the electron detected in the scattering plane (normally called the scattered electron) and the subscript 2 to designate the other electron (normally called the ejected electron) which will be detected in the perpendicular plane for this work. The triple differential cross section for a given orientation $\mathbf{R}$ can be obtained from

$$\sigma^{\rm TDCS}(\mathbf{R}) = \frac{1}{(2\pi)^5}\frac{k_a k_b}{k_i}[|T_{\rm dir}(\mathbf{R})|^2 + |T_{\rm exc}(\mathbf{R})|^2 + |T_{\rm dir}(\mathbf{R}) - T_{\rm exc}(\mathbf{R})|^2]. \quad (2)$$

The exchange T matrix $T_{\rm exc}$ is the same as Eq. (1) except that $\mathbf{r}_1$ and $\mathbf{r}_2$ are interchanged in the final-state wave function.

B. MCM3DW approximation

While the bound-state molecular wave function $\psi_{Dy}(\mathbf{r}_2,\mathbf{R})$ used in the T matrix depends on the orientation of the molecule $\mathbf{R}$, the distorted waves are calculated using spherically symmetric multicenter potentials that contain no information about the molecular orientation. Consequently, it is desirable to replace these distorted waves by wave functions that depend on the molecular orientation as well. Chuluunbaatar *et al.* [24] showed that an orientated wave function called the two-center Coulomb (TCC) produced results in very good agreement with those obtained by a partial-wave treatment of the exact solution of the two-center Schrödinger equation in prolate spheroidal coordinates for the H_2^+ ion [25]. The TCC final-state wave function for H_2^+ is given by (outgoing wave boundary conditions)

$$\chi_{\rm TCC}^+(\mathbf{k},\mathbf{r}) = e^{i\,\mathbf{k}\cdot\mathbf{r}}C_a(\mathbf{k},\mathbf{r}_a)C_b(\mathbf{k},\mathbf{r}_b), \quad (3)$$

where $C_a(\mathbf{k},\mathbf{r}_a)$ is the Coulomb interaction between the ejected electron and nucleus a, $\mathbf{r}_a$ is the distance from nucleus a to the ejected electron, and $C_b(\mathbf{k},\mathbf{r}_b)$ is the equivalent interaction with the other nuclei and the coordinate $\mathbf{r}$ is with respect to the c.m. The vectors relative to the nuclei can be expressed in terms of the c.m. coordinate and orientation vector $\mathbf{R}$ as follows: $\mathbf{r}_a = -\frac{\mathbf{R}}{2} + \mathbf{r}$ and $\mathbf{r}_b = \frac{\mathbf{R}}{2} + \mathbf{r}$.

The Coulomb interaction factor $C_a(\mathbf{k},\mathbf{r}_a)$ is a known analytic function (Gamov factor times a hypergeometric function) which depends on the charge of the nucleus. An important question concerns how this charge should be chosen. If long range interactions are more important than short range, then a logical choice would be to choose each charge as $\frac{1}{2}$ to have a correct net charge asymptotically. On the other hand, if short range interactions are dominant, then a different choice might be appropriate. One of the drawbacks of the TCC wave function lies in the fact that each atom (proton or partially screened proton) has to be represented by an effective point

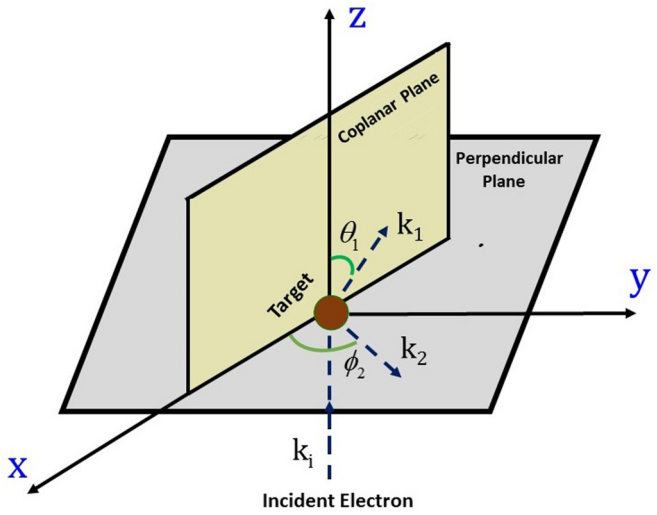

FIG. 1. Coordinate system showing the experimental geometry and variables used in the paper.

charge. One of the primary strengths of the distorted-wave method lies in the fact that the distorting potentials used in the calculation of distorted waves can be considered as radially dependent effective charges. For example, the distorting potential for a neutral hydrogen atom corresponds to an effective charge of $+1$ at the nucleus and this reduces to zero for radii larger than the size of the atom due to the screening of the electron. Consequently, it would be desirable to have a distorted-wave version of the TCC which could have radially dependent effective charges. For analytic Coulomb waves, the connection between the Coulomb wave function $\chi^+_{\rm CW}(\mathbf{k}, \mathbf{r}_a)$ and the Coulomb interaction factor for nuclei a, $C(\mathbf{k}, \mathbf{r}_a)$, is given by (outgoing wave boundary conditions)

$$C(\mathbf{k}, \mathbf{r}_a) = e^{-i\,\mathbf{k}\cdot\mathbf{r}_a}\chi^+_{\rm CW}(\mathbf{k}, \mathbf{r}_a). \tag{4}$$

We propose a generalized numerical interaction (distortion) factor (again outgoing wave boundary conditions) for atom a,

$$D(\mathbf{k}, \mathbf{r}_a) = e^{-i\,\mathbf{k}\cdot\mathbf{r}_a}\chi^+_{\rm DW}(\mathbf{k}, \mathbf{r}_a), \tag{5}$$

where $\chi^+_{\rm DW}(\mathbf{k}, \mathbf{r}_a)$ is a single-center distorted wave with outgoing wave boundary conditions calculated using a numerical distorting potential for atom a and $\mathbf{r}_a$ is the vector from the center of the atom to the continuum electron (i.e., this distortion factor contains the same radially dependent effective charge as was used to calculate the distorted wave). Consequently, the multicenter distorted-wave (MCDW) generalization of the TCC wave function for $H_2{}^+$ would be given by

$$\chi^+_{\rm MCDW}(\mathbf{k}, \mathbf{r}, \mathbf{r}_a, \mathbf{r}_b) = e^{i\,\mathbf{k}\cdot\mathbf{r}}D_a(\mathbf{k}, \mathbf{r}_a)D_b(\mathbf{k}, \mathbf{r}_b), \tag{6}$$

where $D_a(\mathbf{k}, \mathbf{r}_a)$ is the distortion factor between the ejected electron and atom a and $D_b(\mathbf{k}, \mathbf{r}_b)$ is the corresponding distortion factor for atom b. Since $\mathbf{r}_a$ and $\mathbf{r}_b$ can be expressed in terms of $\mathbf{r}$ and $\mathbf{R}$, $\chi^+_{\rm MCDW}(\mathbf{k}, \mathbf{r}, \mathbf{r}_a, \mathbf{r}_b) = \chi^+_{\rm MCDW}(\mathbf{k}, \mathbf{r}, \mathbf{R})$. For practical calculations, one would calculate distorted waves

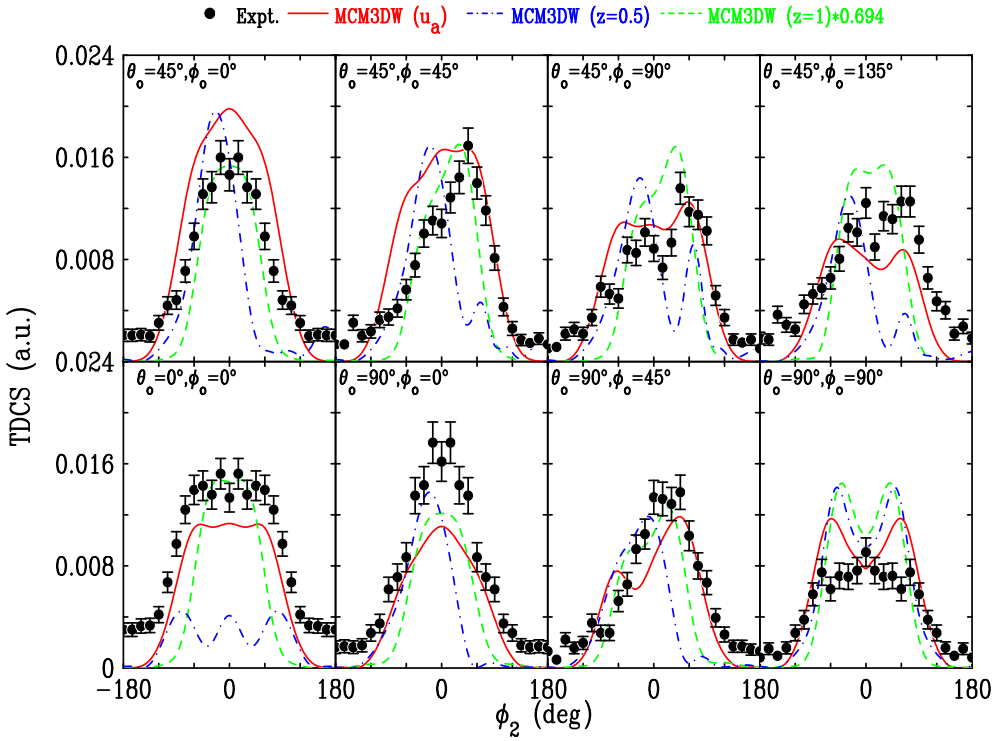

FIG. 2. Comparison of experimental and theoretical TDCS for 54-eV electron-impact ionization of orientated H_2 with the ejected electron being detected in the perpendicular plane at angle ϕ_2. The scattered electron is detected at an angle $\theta_1 = 50^\circ$ in the scattering plane and both final-state electrons have an energy of 18 eV. The experimental data are those of Ren *et al.* [22] and the different panels correspond to different (θ_0, ϕ_0) angles of orientation for the $H_2{}^+$ ion. The theoretical calculations are the three different MCM3DW calculations described in the text. Experiment has been normalized to the MCM3DW(u_a) results with an orientation of ($\theta_0 = 45^\circ$, $\phi_0 = 45^\circ$).

centered on each atom, calculate the distortion factor of Eq. (5), and then transform to the c.m. coordinate system. Consequently, in the MCM3DW approximation, the direct T matrix is given by

$$T_{\rm dir}(\mathbf{R}) = \langle \chi^{-}_{\rm MCDW}(\mathbf{k}_1, \mathbf{r}_1, \mathbf{R}) \chi^{-}_{\rm MCDW}(\mathbf{k}_2, \mathbf{r}_2, \mathbf{R}) C_{12}(\mathbf{r}_{12}) | V_i - U_i | \psi_{Dy}(\mathbf{r}_2, \mathbf{R}) \chi_i^{+}(\mathbf{k}_i, \mathbf{r}_1) \rangle. \quad (7)$$

III. RESULTS

Ren *et al.* [22] reported experimental measurements for ionization of molecular hydrogen in which the orientation of the molecule at the time of ionization was also determined. The measurements were performed for relatively low incident electron energies ranging from 26 to 54 eV, symmetric final-state outgoing electron energies, a fixed scattered electron angle in the scattering plane $\theta_1 = 50^\circ$, and the ejected electron being detected in the perpendicular plane (see Fig. 1). For an incident energy of 54 eV, measurements were performed for several different orientations ranging from the incident beam direction, orientations on a cone centered on the incident beam direction with a half angle of 45°, to orientations in a plane perpendicular to the incident beam direction. Two additional measurements were performed for lower incident electron energies for a fixed orientation in the perpendicular plane. The measurements are relatively absolute such that a single normalization places all the data on an absolute scale.

We have performed calculations for three different models: (1) Both nuclei are treated as point charges $z = 1$; (2) both nuclei are treated as point charges with $z = \frac{1}{2}$; and (3) one nucleus is treated as a neutral hydrogen atom and the other nucleus is treated as a proton with $z = 1$. Cases (1) and (2) correspond to the TCC wave function with different effective charges. For case (3), the distortion factor for one of the nuclei was calculated using a distorted wave obtained from an asymptotically neutral atomic distorting potential (u_a) and the other nucleus is an unscreened proton. We label model (3) calculations as MCM3DW(u_a). For case (1) the residual electron provides no screening, for case (2) the residual electron provides half screening for both protons, and for case (3) the residual electron totally screens one proton and not the other one. For case (1), the net asymptotic charge is not correct while it is correct for cases (2) and (3).

Our MCM3DW results are compared with the experimental data in Fig. 2 for an incident electron energy of 54 eV. For the coordinate system used in Fig. 2, the scattering plane electron is detected at ($\theta_1 = 50^\circ$, $\phi_1 = 180^\circ$), i.e., in the $(-x, +z)$ half plane, and the other electron is ejected in the perpendicular plane ($\theta_2 = 90^\circ$, ϕ_2). The different panels in Fig. 2 correspond to different orientations of the H_2^+ ion. Since we have used the subscripts 1 and 2 for the scattering plane and other plane electron, we will use the subscript 0 for the orientation of the H_2^+ ion. The orientation ($\theta_0 = 0^\circ$, $\phi_0 = 0^\circ$) corresponds to an orientation parallel to the incident beam direction, the top row in Fig. 2 corresponds to different orientations on a cone with a half angle of 45° relative to the incident beam direction, and the bottom three panels on the right-hand side correspond to orientations in the perpendicular plane. As we mentioned above, the experimental data were measured in such a way that a single normalization factor places all the data on an absolute scale. We have chosen this normalization factor by normalizing the experiment to the largest MCM3DW(u_a) cross section with an orientation of ($\theta_0 = 45^\circ$, $\phi_0 = 45^\circ$).

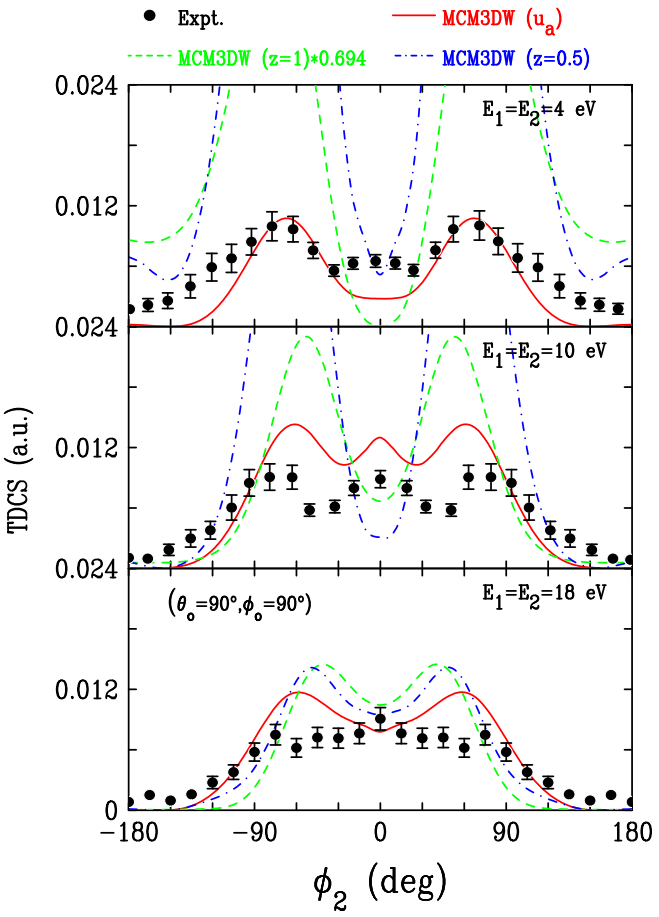

FIG. 3. Comparison of experimental and theoretical TDCS for electron-impact ionization of orientated H_2 with the ejected electron being detected in the perpendicular plane at angle ϕ_2. The scattered electron is detected at an angle $\theta_1 = 50^\circ$ in the scattering plane and both final-state electrons have equal energies as indicated. The experimental data are those of Ren *et al.* [22] and the H_2^+ ion is orientated at ($\theta_0 = 90^\circ$, $\phi_0 = 90^\circ$). The theoretical calculations are the three different MCM3DW calculations described in the text and the normalization factor is the same as that used in Fig. 2.

From Fig. 2, it is seen that model (2) gives the worst agreement with experiment while models (1) and (3) give relatively good agreement with experiment. However, overall, model (3) probably gives the best agreement with experiment. The fact that model (2) where both nuclei are half screened gives the worst agreement suggests that the asymptotic charge is not important and that a charge of $\frac{1}{2}$ near either nucleus is not correct. Close to the nuclei, models (1) and (3) are nearly the same since there is very little screening in that region. The fact that model (1) worked as well as it did suggests that the close interactions are the most important and further confirms the conclusion that asymptotic net charge is not important.

Figure 3 compares the MCM3DW results with experiment for three different incident electron energies and a fixed orientation of ($\theta_0 = 90^\circ$, $\phi_0 = 90^\circ$). Here the normalization is

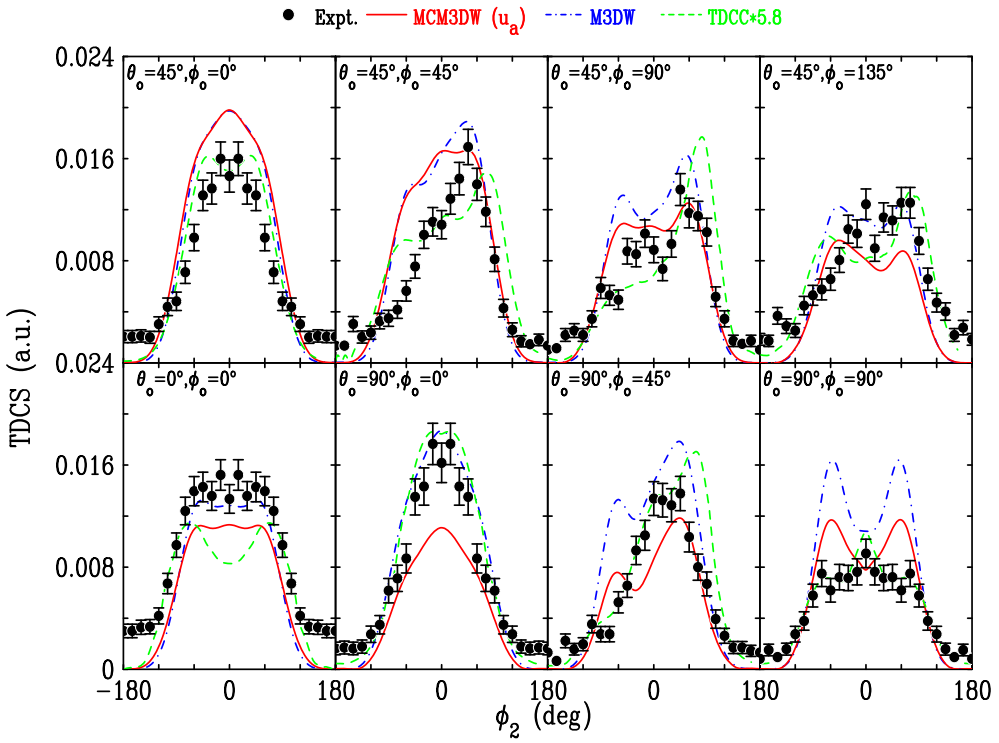

FIG. 4. Comparison of experimental and theoretical TDCS for 54-eV electron-impact ionization of orientated H_2 with the ejected electron being detected in the perpendicular plane at angle ϕ_2. The experimental data are those of Ren *et al.* [22] and the different panels correspond to different (θ_0, ϕ_0) angles of orientation for the H_2^+ ion. The theoretical calculations are the MCM3DW (u_a) (solid red curve), the M3DW (dashed-dot blue curve), and the TDCC (dashed green). The normalization factor is the same as that used in Fig. 2.

the same as Fig. 2 and the $E_1 = E_2 = 18$ eV results are the same in Figs. 2 and 3. Here it is seen that the MCM3DW (u_a) results are in relatively good agreement with experiment while the magnitudes of the cross section for the other two models significantly overestimate the experimental data for the lower incident electron energies and the overestimation becomes larger as the energy decreases.

Figure 4 compares the MCM3DW (u_a) [model (3)] results with M3DW results for which the continuum distorted waves do not depend on the orientation of the molecule. Interestingly, the two calculations are very similar in shape with the largest differences occurring for the magnitude of the cross section which indicates that the orientation of the H_2^+ ion does not play an important role in determining the shape of the TDCS. It is also interesting to note that when there is a noticeable difference between the two calculations, the M3DW results are in better agreement with the magnitude of the experiment than the MCM3DW for most cases. In the M3DW, the H_2^+ ion continuum wave functions are calculated using a spherically symmetric potential. Although this potential is spherically symmetric, it nonetheless contains the multicenter information since it is formed from both the nuclear and electronic contributions. Taking a spherical average for any nucleus in a molecule places the nuclear charge on a very thin spherical shell whose radius is the distance of the nucleus from the c.m. Since H_2 has two protons an equal distance from the c.m., the nuclear contribution consists of a charge of $+2$ located on a thin spherical shell with radius $r = 0.7\ a_0$. For the electronic contribution, the charge distribution obtained from the numerical wave functions calculated using density functional theory is used to calculate the effective radially dependent screening. The fact that the M3DW results predicts the magnitude of the cross section somewhat better than the MCM3DW suggests that this potential yields a better continuum wave function than the product of two atomic wave functions, at least for 18-eV-energy ejected electrons.

The next question concerns why the MCM3DW (u_a) model is so similar to the M3DW since the ejected electron "sees" a spherically symmetric potential in the M3DW and an orientation-dependent potential in the MCM3DW. The potential used for the MCM3DW (u_a) has a proton located at $r = 0.7\ a_0$ from the c.m. at a point determined by the orientation and another proton located at $r = 0.7\ a_0$ on the opposite side of the c.m. One of these protons has a spherically symmetric charge distribution for an electron centered on the proton. For the M3DW, there is a spherically symmetric charge distribution for an electron centered on the c.m. and a charge of $+2$ located on a sphere of radius $r = 0.7\ a_0$. The similarity of the two cross sections indicates that, with increasing ejected electron energy, the $r = 0.7\ a_0$ offset of the charge distribution and exact location of the protons becomes less important.

Figure 4 also contains the TDCC results reported in Ren *et al.* [22]. The TDCC results are multiplied by a factor of 5.8 to obtain the same relative comparison with experiment as seen in Ren *et al.* [22]. There are cases where the TDCC is closer to experiment than the M3DW and some cases where the M3DW results are in somewhat better agreement with experiment. For the orientation ($\theta_0 = 90°$, $\phi_0 = 45°$), M3DW and MCM3DW results exhibit some structure that is not seen

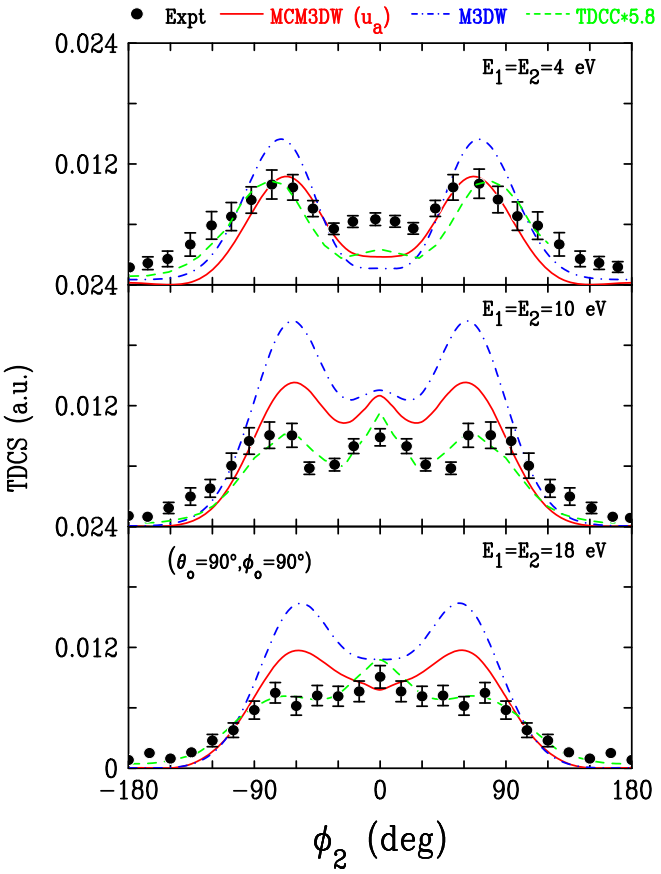

FIG. 5. Comparison of experimental and theoretical TDCS for electron-impact ionization of orientated H_2 with the ejected electron being detected in the perpendicular plane at angle ϕ_2. Both final-state electrons have equal energies as indicated. The experimental data are those of Ren *et al.* [22] and the H_2^+ ion is orientated at ($\theta_0 = 90^\circ$, $\phi_0 = 90^\circ$). The theoretical calculations are the MCM3DW (u_a) (solid red curve), the M3DW (dashed-dot blue curve), and the TDCC (dashed green). The normalization factor is the same as that used in Fig. 2.

in either the experiment nor TDCC [although the structure is seen in all three theories and experiment for ($\theta_0 = 45^\circ$, $\phi_0 = 90^\circ$)]. Also, for ($\theta_0 = 90^\circ$, $\phi_0 = 90^\circ$), the two M3DW results have a minimum at $\phi_2 = 0^\circ$ while both experiment and the TDCC have a maximum. On the other hand, experiment indicates that the two peaks around $\phi_2 = 60^\circ$ are probably correct. With the two noted exceptions for orientations in the perpendicular plane, the TDCC and the M3DW are both in about the same level of agreement with experiment.

Figure 5 compares the above three calculations with experiment for three different incident electron energies and a fixed orientation of ($\theta_0 = 90^\circ$, $\phi_0 = 90^\circ$). It is seen that, for decreasing incident electron energy, the MCM3DW (u_a) results are in better agreement with experiment than the M3DW. For the 10-eV case, all three theories predict a peak for $\phi_2 = 0^\circ$. Whereas the TDCC is in better agreement with experiment for the two higher energies, the TDCC and MCM3DW (u_a) results are in about the same level of agreement for the lowest energy. It may seem surprising that a perturbation series calculation can yield such good agreement with experiment for

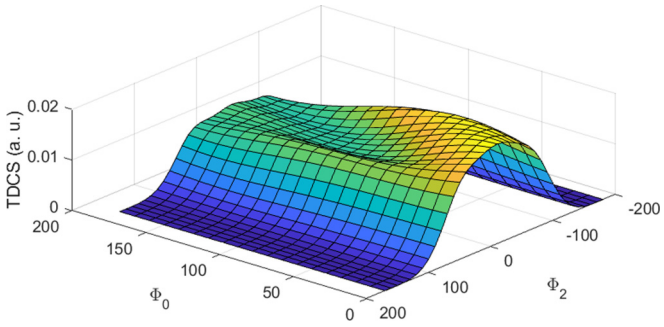

FIG. 6. Theoretical M3DW TDCS for 54-eV electron-impact ionization of orientated H_2 with the ejected electron being detected in the perpendicular plane at angle ϕ_2. The H_2^+ ion is orientated along a cone with a half angle of $\theta_0 = 45^\circ$ and ϕ_0 is the azimuthal angle on the cone.

such a low energy. The fact that this is possible can be traced to the Coulomb interaction factor $C_{12}(\mathbf{r}_{12})$ that is included in the approximation for the final-state wave function. It is well known that any physics that is contained in the wave function is automatically contained to all orders of perturbation theory so PCI is included to infinite order. In the present case, both final-state electrons have equal energies which maximizes the importance of PCI. We have previously shown that the M3DW approach is valid even all the way down to threshold when PCI is important so it is not surprising that the theory could work this well for the lowest energy.

Next we investigate the origin of the M3DW structure not seen in experiment. To investigate how the TDCS change for different orientations, we have performed a series of calculations in which we keep the orientation angle θ_0 fixed and vary ϕ_0 (i.e., examine how the cross section changes for orientations aligned along a cone of half angle $\theta_0 = 45^\circ$ and $\theta_0 = 90^\circ$). Figure 6 shows a surface plot for the $\theta_0 = 45^\circ$ cone. From the figure, it is seen that the large peak located at $\phi_2 = 0^\circ$ develops into a minimum which is also reflected in the experimental data (three right-hand panels of Figs. 2 and 4).

The surface plot for $\theta_0 = 90^\circ$ (molecular orientation also in the perpendicular plane) is shown in Fig. 7. There is a lot of symmetry in this plane. For example, $\phi_0 = 0^\circ$ and 180° have

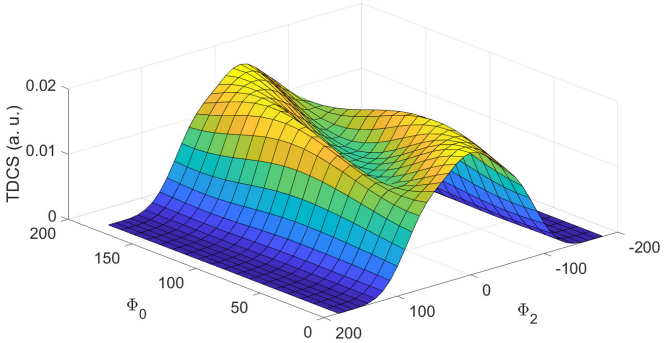

FIG. 7. Theoretical M3DW TDCS for 54-eV electron-impact ionization of orientated H_2 with the ejected electron being detected in the perpendicular plane at angle ϕ_2. The H_2^+ ion is orientated in the perpendicular plane as well ($\theta_0 = 90^\circ$) and ϕ_0 is the azimuthal angle in the plane.

to be the same and they both are symmetrical about $\phi_2 = 0^\circ$. Also the $\phi_0 = 90^\circ$ TDCS must be symmetrical about $\phi_2 = 0^\circ$. The two predicted surfaces for the $\theta_0 = 45^\circ$ and $\phi_0 = 90^\circ$ cones are similar except that the 90° cone exhibits more structure. The structure seen for ($\theta_0 = 90^\circ$, $\phi_0 = 45^\circ$) and ($\theta_0 = 90^\circ$, $\phi_0 = 90^\circ$) can now be traced to the valley located between the two hills. Since the experimental data for ($\theta_0 = 90^\circ$, $\phi_0 = 90^\circ$) suggest a center peak with two side peaks, it appears that there should be a ridge in the middle of the valley that is not predicted by the M3DW. The experimental data for ($\theta_0 = 90^\circ$, $\phi_0 = 45^\circ$) suggest that a valley is just starting to be formed at $\phi_0 = 45 (\theta_0 = 90^\circ$, $\phi_0 = 90^\circ$) whereas the valley forms sooner in the M3DW.

IV. CONCLUSIONS

We have previously used the molecular three-body distorted-wave (M3DW) model to examine electron-impact single ionization of molecules. Although the orientation of the molecule is taken into account in the initial-state molecular wave function in this model, the continuum electron wave functions do not depend on the orientation and this was considered to be a potential problem with the model. Consequently, here we introduced a continuum electron distorted wave which does depend on the orientation. This wave function is basically a product of distorted waves for each atom in the molecule (in this case, two hydrogen atoms) modified to properly satisfy the required asymptotic boundary conditions of an incoming or outgoing wave. The multicenter molecular three-body distorted-wave (MCM3DW) results were compared with experimental data taken by Dorn and colleagues in Heidelberg, Germany [4,5,16,20,22], for which they measured triple differential cross sections (TDCS) for single ionization of molecular hydrogen while simultaneously determining the orientation of the H_2^+ ion at the time of ionization since such an experiment would represent the most sensitive test of the treatment of molecular orientation in a theoretical calculation.

The potential used to calculate distorted waves contains a nuclear contribution and an electron contribution which effectively provides a radially dependent screening. What is not clear is how this screening would be shared between the two protons after ionization. Consequently, we tried three different models: (1) no screening so that each distorted wave is simply a Coulomb wave for charge unity; (2) equal shared screening so that each atom can be approximated by an effective charge of $\frac{1}{2}$; (3) an electron attached to one of the protons so that there is effectively a proton and a neutral hydrogen atom. Of the three models, model 2 gave the worst agreement with experimental data which suggest that the asymptotic net charge is not important and an effective charge of $\frac{1}{2}$ is not appropriate for close collisions. Models (1) and (3) gave similar results in reasonable agreement with experiment for the highest energy considered. For small radii, the effective screened potential for neutral hydrogen is close to unity so both models have similar effective charges for small radii. This observation further supports the suggestion that asymptotic net charges are not important but that close collisions dominate the results. For the two lower energies, model (3) was in significantly better agreement with experiment.

The model (3) MCM3DW results were compared with M3DW results and it was found that, in terms of shape, the differences between the two calculations were small. However, for the higher-energy 18-eV ejected electrons, the M3DW predicted the magnitude of the cross section better than the MCM3DW (u_a). This suggests that the screening contained in the distorting potential used for the M3DW calculation is a better approximation than the screening contained in the MCM3DW (u_a) calculation, at least in terms of getting the magnitude of the cross section correct. For the case of the two lower-energy ejected electrons, the MCM3DW (u_a) results were in better agreement with experiment that the M3DW. This suggests that orientation plays a more important role as the incident electron energy decreases but is less important by the time the incident electron energy is 54 eV. We also compared the present results with the TDCC. For the highest-energy cases, both the M3DW and TDCC were in about the same level of agreement with experiment. However, for the 10-eV case, the TDCC was in better agreement with experiment while the TDCC and MCM3DW (u_a) were in about the same level of agreement for the 4-eV case.

Finally we examined how the TDCS changed as a function of the orientation of the H_2^+ ion for orientations aligned along cones of half angles of 45 ($\theta_0 = 90^\circ$, $\phi_0 = 90^\circ$) and 90° centered on the incident beam direction. It was found that the maximum cross sections occurred opposite the direction of the scattering plane electron and decreased when rotated towards the direction of the scattering plane electron. In both cases, the peak located at $\phi_2 = 0 (\theta_0 = 90^\circ$, $\phi_0 = 90^\circ$) developed into a valley with increasing ϕ_0. For the $\theta_0 = 45 (\theta_0 = 90^\circ$, $\phi_0 = 90^\circ$) cone, there was reasonably good agreement between experiment and the M3DW. For the $\theta_0 = 90 (\theta_0 = 90^\circ$, $\phi_0 = 90^\circ$) cone, the M3DW predicted the formation of a valley at a smaller ϕ_0 than seen in experiment.

ACKNOWLEDGMENT

The authors would like to thank one of the referees who suggested the explanation for why the MCM3DW (u_a) converges to the M3DW for increasing ejected electron energies.

[1] I. Bray and A. T. Stelbovics, Phys. Rev. A **46**, 6995 (1992).
[2] J. Colgan and M. S. Pindzola, Phys. Rev. A **74**, 012713 (2006).
[3] T. N. Rescigno, M. Baertschy, W. A. Isaacs, and C. W. McCurdy, Science **286**, 2474 (1999).
[4] X. Ren, S. Amami, O. Zatsarinny, T. Pfluger, M. Weyland, W. Y. Baek, H. Rabus, K. Bartschat, D. Madison, and A. Dorn, Phys. Rev. A **91**, 032707 (2015).
[5] X. Ren, S. Amami, O. Zatsarinny, T. Pflüger, M. Weyland, A. Dorn, D. Madison, and K. Bartschat, Phys. Rev. A **93**, 062704 (2016).
[6] M. Zammit, J. Savage, D. Fursa, and I. Bray, Phys. Rev. Lett. **116**, 233201 (2016).
[7] D. Gorfinkiel and J. Tennyson, J. Phys. B **38**, 1607 (2005).

[8] M. S. Pindzola, F. Robicheaux, S. D. Loch, and J. P. Colgan, Phys. Rev. A **73**, 052706 (2006).
[9] J. Colgan, M. S. Pindzola, F. Robicheaux, C. Kaiser, A. J. Murray, and D. H. Madison. Phys. Rev. Lett. **101**, 233201 (2008).
[10] J. Colgan, O. Al-Hagan, D. H. Madison, C. Kaiser, A. J. Murray, and M. S. Pindzola, Phys. Rev. A **79**, 052704 (2009).
[11] D. H. Madison and O. Al-Hagan, J. At., Mol. Opt. Phys. **2010**, 367180 (2010).
[12] J. Gao, D. H. Madison, and J. L. Peacher, J. Chem. Phys. **123**, 204314 (2005).
[13] J. Gao, D. H. Madison, and J. L. Peacher, Phys. Rev. A **72**, 032721 (2005).
[14] J. Gao, D. H. Madison, and J. L. Peacher, J. Chem. Phys. **123**, 204302 (2005).
[15] E. Ali, K. Nixon, A. J. Murray, C. Ning, J. Colgan, and D. H. Madison, Phys. Rev. A **92**, 042711 (2015).
[16] M. Gong, X. Li, S. B. Zhang, S. Niu, X. Ren, E. Wang, A. Dorn, and X. Chen, Phys. Rev. A **98**, 042710 (2018).
[17] N. Sanna and F. Gianturco, Comput. Phys. Commun. **128**, 139 (2000).
[18] N. Sanna and G. Morelli, Comput. Phys. Commun. **162**, 51 (2004).
[19] N. Sanna, I. Baccarelli, and G. Morelli, Comput. Phys. Commun. **180**, 2544 (2009).
[20] X. Ren, S. Amami, K. Hossen, E. Ali, C. Ning, J. Colgan, D. Madison, and A. Dorn, Phys. Rev. A **95**, 022701 (2017).
[21] S. J. Ward and J. H. Macek, Phys. Rev. A **49**, 1049 (1994).
[22] X. Ren, T. Pflüger, S. Xu, J. Colgan, M. S. Pindzola, A. Senftleben, J. Ullrich, and A. Dorn, Phys. Rev. Lett. **109**, 123202 (2012).
[23] O. Al-Hagan, C. Kaiser, D. Madison, and A. Murray, Nat. Phys. **5**, 59 (2009).
[24] O. Chuluunbaatar, B. Joulakian, Kh. Tsookhuu, and S. I. Vinitsky, J. Phys. B **37**, 2607 (2004).
[25] V. V. Serov, B. Joulakian, V. L. Derbov, and S. I. Vinitsky, J Phys. B **38**, 2765 (2005).